NUMERICAL EXPERIMENTS TO EVALUATE EFFECT OF EXTERNAL FORCES ON TEMPERATURE STRATIFICATION IN LAKE KASUMIGAURA, JAPAN

WANG YUEYI
Department of Civil Engineering, Graduate School of Engineering, Osaka University, Suita, Japan, yueyi@civil.eng.osaka-u.ac.jp

MASAYASU IRIE
Department of Civil Engineering, Graduate School of Engineering, Osaka University, Suita, Japan, irie@civil.eng.osaka-u.ac.jp

SHUNSUKE KOMURO
Ibaraki Kasumigaura Environmental Science Center, Tsuchiura, Japan, sh.komuro@pref.ibaraki.lg.jp

GUILLAUME AUGER
IBM T.J. Watson Research Center, New York, United States, Guillaume.Auger@ibm.com

AYATO KOHZU
National Institute for Environmental Studies, Tsukuba, Japan, kohzu@nies.go.jp

ABSTRACT

Lake Kasumigaura is the second largest lake in Japan, and it is shallow and highly eutrophic. Although variations in lake current have been revealed by field observations in previous research, numerical simulations should be adopted to further reveal the influence of external forces on the lake flow, and investigate the phenomena of temperature stratification and algal blooms. An unstructured grid, parallel computing coastal ocean model, SUNTANS, is utilized for modeling lake currents in this study. The horizontal resolution of the unstructured grid is approximately 200 m, and 30 layers are split vertically. The simulation results demonstrated that SUNTANS could reproduce observations in the lake and had a good performance for modeling the obvious diurnal stratification. Through a comparison of results of different cases, the difference in the temporal temperature change would indicate the driving effect of wind and the significant contribution of insolation to the formation of stratification. Particle-tracking results showed a strong relationship between the surface distribution of algal blooms and the wind condition. Wind driving combined with topographic conditions led to a tendency for particles to become trapped by a complicated shoreline and accumulate on the northern part of the lake. This trend was inferred to be one of the reasons why algal blooms often occur in those areas.

Keywords: *Unstructured grid, wind driven current, diurnal temperature stratification, Lake Kasumigaura, SUNTANS*

1. INTRODUCTION

Once a lake is formed, it will evolve continuously by external natural factors and various internal processes. The main difference between natural and anthropogenic eutrophication is that the natural process is very slow, occurring on geological time scales (Callisto et al., 2014). Human interference can significantly accelerate lake eutrophication. Hypoxia is a phenomenon occurring in the aquatic environment usually as a result of eutrophication and stratification. Some reporters have declared that when dissolved oxygen (DO) concentration is below 4.3 mg/L, bottom-dwelling fish and crustaceans begin to show a tendency to disappear, and the lethal level of DO for fish with weak oxygen tolerance is approximately 3.0 mg/L (Sasaki, 1993). If hypoxia occurs, fisheries in the region will face significant losses (Doudoroff and Shumway, 1970). Therefore, it is important to study the characteristics of flow in temperature-stratified water to understand the formation, development, and disappearance processes of hypoxia in temperature-stratified lakes.

Water-temperature stratification has a large impact on the algal blooms and the emergence of hypoxic water masses. Understanding the water flow patterns of lakes is central to understanding and solving water quality problems. Only existing field survey data, however, sometimes are not enough to reveal the characteristics of the flow and to determine the leading factors driving hypoxia due to their spatial and temporal resolution. Even though at present and in the near future, the 1D model with its extremely efficiency will remain the primary method for simulating temperature changes in lake water (Belolipetsky et al., 2010, Stepanenko et al., 2014, Thiery et al., 2014) but 3D Model provides better resolution of topographical effects, internal waves, mixing, and spatial gradients of environmental forcing (Jin et al., 2000, Kimura et al., 2016). However, a long-

term 3D lake dynamics simulation requires increasing available computational speed and memory. Therefore, this study applied a 3D model into a short-term simulation to gain a greater understanding of transport processes.

The Stanford Unstructured Nonhydrostatic Terrain-Following Adaptive Navier–Stokes Simulator (SUNTANS) is a relatively advanced unstructured grid flow model (Fringer et al., 2006), which is commonly used worldwide. Chua and Fringer (2011) applied SUNTANS to San Francisco Bay, and the results showed that the model accurately predicted tidal heights, currents, and salinity at several locations throughout the Bay. Rayson et al. (2015) tested three different unstructured meshes and declared that salinity and sub-tidal velocity were better predicted when the important topographic features, such as the shipping channel, were resolved. In Japan, some research groups have begun to use SUNTANS for simulation studies. It has been used to investigate river plume mixing in Otsuchi Bay by Masunaga et al. (2016), concluding that all barotropic and baroclinic tides and wind are important for mixing processes. However, most of the studies have focused on simulation in estuaries and coastal seas.

In this study, based on observations, a numerical simulation was conducted to reveal the stratification structure due to thermal gradient and wind stress. The calculation results also demonstrate how external forces effect the hypoxia variations in Lake Kasumigaura, Japan (Figure 1). Komatsu et al. (2010) revealed the strong relationship between the phenomena of hypoxia with the vertical distribution of water temperature by field observations. Kitazawa et al. (2008) applied a three-dimensional model to the lake, which shows excellent reproducibility of water temperature. However, to better simulate the vertical stratification and the temporal temperature change, setting precise boundary conditions is necessary. This study analyzes the effects of external forces on the flow characteristics of the lake founded on the observation data and the simulation by the unstructured grid, three-dimensional flow model. This study follows the approach of Auger and Wells (2016), who studied the influence of a typhoon on gyre generation in Lake Biwa, Japan using the same model.

2. STUDY AREA

The research area is located in the east-central Japan, approximately 60 km from Tokyo, as shown in Figure 1.

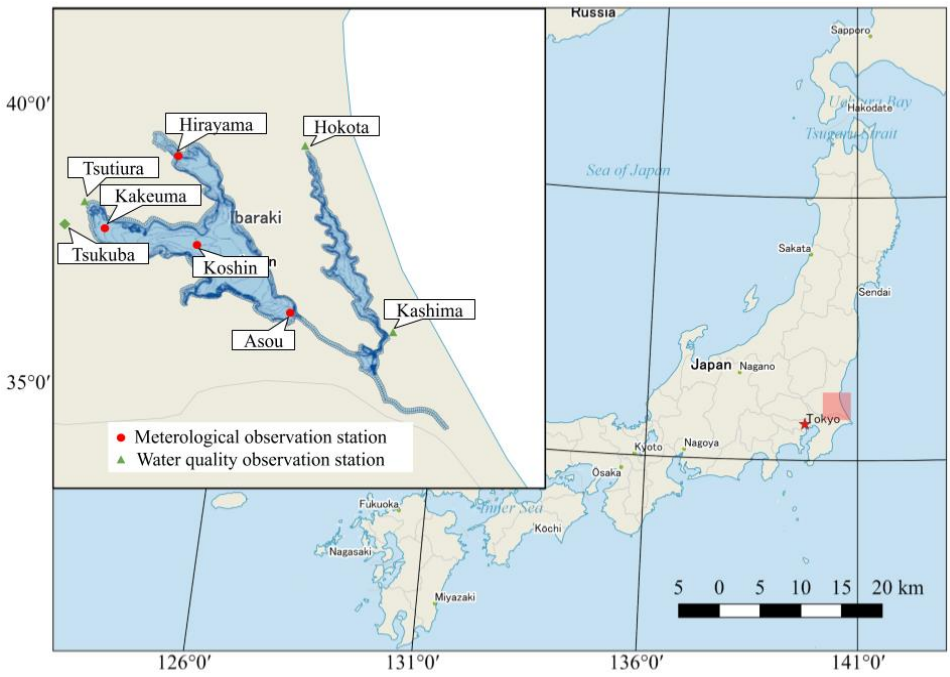

Figure 1. Geographical location and plane shape of Lake Kasumigaura. The red circles show the location of water quality stations, while the green marks indicate the location of meteorological stations.

The lake refers to a group of adjacent lakes and can be roughly divided into three parts: Nishiura in the west (167.63 km^2), Kitaura in the east (35.16 km^2), and Sotonasakaura, a small southern part (5.85 km^2), and it includes the rivers connecting them. Lake Kasumigaura is the second largest in Japan with a total area of approximately 220 km^2, which is a representative of shallow eutrophication lakes. Although the plane shape is somewhat complicated, the average depth of the lake is about 4 m, and its bathymetry is roughly flat and basin-shaped. Additionally, the lake is now almost completely freshwater, owing to a water gate in the lower reaches of the Hitachi Tone River. Therefore, water density is determined only by temperature. Because of its topographic features, it is reasonable to assume that the lake would be significantly affected by external forces such as inflows, insolation, and wind.

Table 1. Basic information of Lake Kasumigaura.

Specification	Value	Remarks
Total area	220 km^2	Lake Nishiura 167.63 km^2, Lake Kitaura 35.16 km^2, Lake Sotonasakaura and other 15.3 km^2
Total coastal line length	250 km	Lake Nishiura 121.4 km, Lake Kitaura 63.9 km, Lake Sotonasakaura and other 64.6 km
Total capacity	850 10^6 m^3	
Maximum Depth	23.8 m	7 m at the Koshin Station, average depth 4 m
Flushing time	Around 200 days	

reference from: https://www.pref.ibaraki.jp/soshiki/seikatsukankyo/kasumigauraesc/04_kenkyu/kasumigaura/kasumigaura.htm

3. METHODOLOGY

3.1 Observations

Figure 1 shows the specific locations of observation stations. The water quality data were collected as a part of the Lake Kasumigaura long-term environmental monitoring program by the National Institute for Environmental Studies (NIES), Japan. The monitoring data contain four automatic observation stations located in Hirayama, Kakeuma, Koshin, and Asou as shown in red circles in Figure 1. These data include water temperature, pH, DO, turbidity, conductivity, chemical oxygen demand (COD), total nitrogen (T-N), total phosphorus (T-P), and chlorophyll, measured hourly from 2008 to 2015. Due to periodic equipment inspection and other reasons, missing data exist in some periods. It should be noted that the Koshin and Asou stations have both surface and bottom data, while other observation sites have only surface data.

Meteorological data are collected from four meteorological observatories surrounding the lake. All data were measured hourly as a part of AMeDAS, which is managed by the Japan Meteorological Agency (JMA). The observation stations are shown by the green triangles in Figure 1. Because the stations have only precipitation, atmospheric temperature, and wind speed and direction data, a larger observation station shown as a green diamond in Figure 1 and closest to the lake, was selected for additional data sources, and contributes short wave, air pressure, humidity, and cloud conditions. The local wind in summer are characterized by weaker morning wind, temporary suspension at noon and strong winds in the evening that continue to blow even in the middle of the night. The frequent strong easterly winds in the lake area is mainly the sea breeze coming from the direction of Kashima beach.

3.2 Model setup

SUNTANS has been implemented to solve the hydrodynamic and transport equations in the present study. It is a non-hydrostatic, parallel coastal ocean model with an unstructured grid system. Although this model has been developed for non-hydrostatic simulation, it is used for various analyses including this study without this strong advantage. Most of the simulation results, however, due to the merits by coordinate systems, show that SUNTANS maintains reproducibility of flow and density with high resolution in estuaries and coastal seas.

3.2.1 Governing equations

SUNTANS uses the Boussinesq approximation and incompressibility assumption ($\nabla \cdot \mathrm{u} = 0$) to solve the Reynolds Averaged Navier-Stokes equation:

$$\frac{\partial u}{\partial t} + \nabla \cdot (\boldsymbol{u}u) - fv + bw = -\frac{1}{\rho_0}\frac{\partial p}{\partial x} + \nabla_H \cdot (v_H \nabla_H u) + \frac{\partial}{\partial z}\left(v_V \frac{\partial u}{\partial z}\right), \quad (1)$$

$$\frac{\partial v}{\partial t} + \nabla \cdot (\mathbf{u}v) + fu = -\frac{1}{\rho_0}\frac{\partial p}{\partial y} + \nabla_H \cdot (v_H \nabla_H v) + \frac{\partial}{\partial z}\left(v_V \frac{\partial v}{\partial z}\right), \quad (2)$$

$$\frac{\partial w}{\partial t} + \nabla \cdot (\mathbf{u}w) - bu = -\frac{1}{\rho_0}\frac{\partial p}{\partial z} + \nabla_H \cdot (v_H \nabla_H w) + \frac{\partial}{\partial z}\left(v_V \frac{\partial w}{\partial z}\right) - \frac{g}{\rho_0}(\rho_0 + \rho). \quad (3)$$

Coriolis terms are given by $f = 2\omega\sin/\emptyset$ and $b = 2\omega\cos/\emptyset$, where ω is the Earth's angular velocity, and ∅ is latitude. The horizontal and vertical eddy viscosities are given by v_H and v_V.

The free surface h is obtained by solving the depth-integrated continuity equation:

$$\frac{\partial h}{\partial t} + \frac{\partial}{\partial x}\left(\int_{-d}^{h} u\, d_z\right) + \frac{\partial}{\partial y}\left(\int_{-d}^{h} v\, d_z\right) = 0, \quad (4)$$

where we have employed kinematic boundary conditions at surface and bottom:

$$\frac{\partial h}{\partial t} + u_H \,/_{z=h} \cdot \nabla_H h = w \,/_{z=h} \quad (5)$$

$$-u_H\ /_{z=-d} \cdot \nabla_H d = w\ /_{z=-d}. \quad (6)$$

After employing a scalar diffusivity law, the transport equations for salinity and temperature are given by

$$\frac{\partial s}{\partial t} + \nabla \cdot (\mathbf{u}s) = \nabla_H \cdot (\gamma_H \nabla_H s) + \frac{\partial}{\partial z}\left(\gamma_V \frac{\partial s}{\partial z}\right), \quad (7)$$

$$\frac{\partial T}{\partial t} + \nabla \cdot (\mathbf{u}T) = \nabla_H \cdot (\kappa_H \nabla_H T) + \frac{\partial}{\partial z}\left(\kappa_V \frac{\partial T}{\partial z}\right), \quad (8)$$

where γ_H, γ_V, κ_H, and κ_V are the horizontal and vertical turbulent mass and thermal diffusivities, respectively.

The vertical viscosity and diffusivity are computed with the Mellor–Yamada level 2.5 (MY2.5) closure scheme (Mellor and Yamada, 1982), with stability functions modified by Galperin et al. (1988). MY2.5 equations are shown as follows:

$$\frac{\partial k}{\partial t} + \bar{u}_i \frac{\partial k}{\partial x_i} = \frac{\partial}{\partial_z}\left(qlS_q \frac{\partial k}{\partial z}\right) + P + B - \varepsilon \quad (9)$$

$$\frac{\partial kl}{\partial t} + \bar{u}_i \frac{\partial (kl)}{\partial x_i} = \frac{\partial}{\partial_z}\left(qlS_q \frac{\partial (kl)}{\partial z}\right) + l(0.9P + 0.9B - 0.5\varepsilon). \quad (10)$$

3.2.2 Initial condition

The computational domain spans from the northernmost Koise River mouth and the Sakura River located at the west end to a water gate built in the lower reaches of the Hitachi Tone River at the southeast end. The major watercourses are the Sakura River and Koise River, which drain into Nishiura, and the Tomoe River and Hokota River, which feed into Kitaura. Table 2 lists the basin area (km^2) and annual averages of river discharges (m^3/s) (shown in parentheses) flowing into the lake in 2008 (the Ibaraki Kasumigaura Environmental Science Center). The smaller rivers are not considered. Only four inflow rivers are treated as upstream open boundaries on the north and west areas, while the lake water outflow to the Hitachi Tone River is the only downstream boundary. The inflows are measured hourly, and a constant depth of 1 m is assumed for the river mouth.

Table 2. Main influent of Kasumigaura.

Tsutiura (Nishiura)	Sakura* 350.30(10.18) Bizen 3.70(0.10)	Sakai 17.44(0.46) Seimei 25.50(0.85)	Nitsu 15.60(0.41) Kawashiri 9.02(0.24)
Takahama (Nishiura)	Koise* 212.60(5.85) Kamata 16.60(0.44)	Sanno 12.30(0.32) Hishiki 23.70(0.62)	Sonobe 79.30(2.08)
North part of Kitaura	Hokota* 41.6(1.83) Daiyo 3.40(0.12)	Tomoe* 131.80(3.27) Daiennji 6.80(0.24)	Nagamo 6.40(0.22) Naganoe 6.60(0.23)
South part of Kitaura	Nakasato 8.10(0.28)	Nagare 3.60(0.12)	Gantsu 8.20(0.28)

* denotes the inflow rivers considered in this study.

The unstructured grid for the domain shown in Figure 2 was generated using SMS (Environmental Modelling Systems, Inc.). The average resolution of the grid, based on triangular cell lengths, is 200 m. In the vertical direction, the grid has structured z-levels, with a maximum of 30 layers in the deepest portion of the domain. The total number of cells horizontally is approximately 8000 and the three-dimensional grid has approximately 166,400 grid cells. The model uses bathymetric data obtained from the Geospatial Information Authority of Japan (GSI).

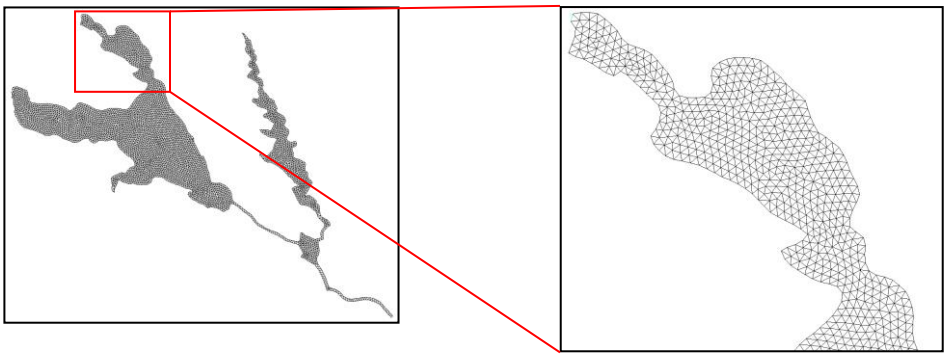

Figure 2. The entire domain is shown in the left-hand figure. The right-hand figure is the refinement at the north part of Nishiura to show the arrangement of the grids.

The simulation is initialized with a flat free surface and a quiescent velocity field. Both inflows and initial lake salinity are assumed to be 0.01 psu, because Lake Kasumigaura is now basically a freshwater lake. The water temperature field in the lake was initialized with the NIES long-term observations starting from January 1, 2008. The data set consists of vertical profiles of water temperature at the surface and bottom layers. It has been interpolated by depth and applied to the cell centers of the grid throughout the lake.

The research period begins from 09/01/2010 to 09/31/2010, because according to the observed data, the hypoxia phenomenon was most obvious during that period. To eliminate the effects caused by the idealized initial condition setting, a preconditioning calculation from 07/01/2010 to 08/31/2010 was added. Table 3 summarizes the details of the calculation conditions.

Table 3. Calculation conditions.

Grid size	Horizontal Average Interval: 200 m Vertical: 30 layers	
Research period	09/01/2010–09/31/2010	
Input data	Precipitation, atmospheric temperature, wind speed and direction, short wave, air pressure, humidity, and cloud conditions.	
Boundary condition	Inflow	4 major rivers
	Outflow	The Hitachi Tone River
Initial condition	Water temperature	

To study the effects of various external forces on the lake, three different cases were simulated using the different external force cases shown in Table 4. All external forces presets are made from observation data. The existence of solar radiation and wind can be achieved by creating different input nc files.

Table 4. Forcing scenarios of Lake Kasumigaura simulation.

	Inflow	**Insolation**	**Wind**
Case-FSW	◎	◎	◎
Case-FS	◎	◎	
Case-FW	◎		◎
Case-SW		◎	◎

4. RESULTS AND DISCUSSION

4.1 Model validation

Two evaluation indices RMSE and R^2 were calculated to validate the model performance using the following formula:

$$RMSE = \sqrt{\frac{1}{m}\sum_{i=1}^{m}(obs_i - cal_i)^2}\,,\ R^2 = 1 - \frac{\sum_i (obs - cal)^2}{\sum_i (mean - obs)^2}. \tag{11}$$

Figure 3 shows the correlation between the calculated and observed temperature at the observation stations. It can be seen from Figure 3 that the blue dots are close to the red diagonal line; combined with the evaluation index, we can say that the water temperature performance of the SUNTANS model is satisfactory.

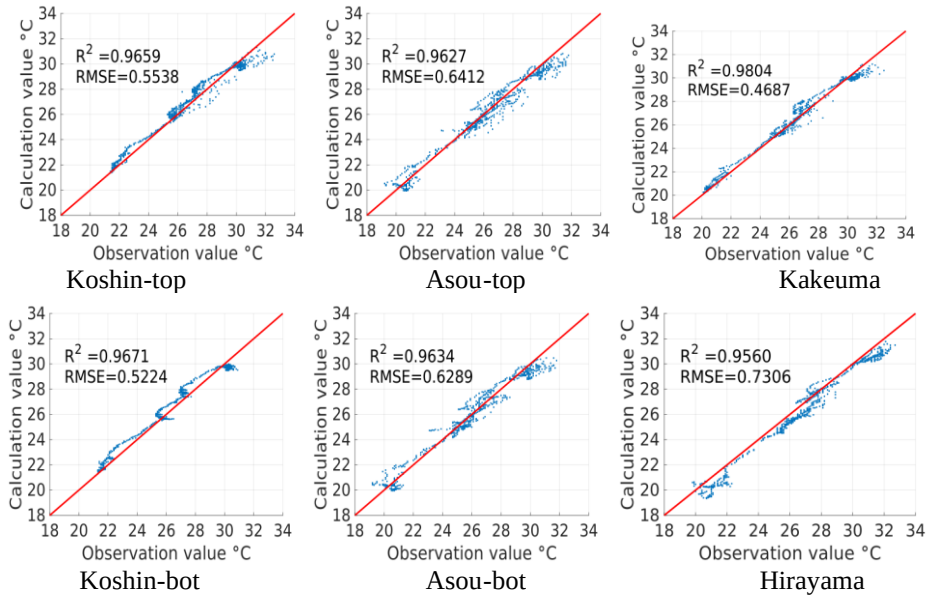

Figure 3. Correlation of calculated results and observed data at Koshin.

As shown in Figure 4, the water temperature at Koshin Station is validated with observed data from 09/01–10/01 in 2010. The result shows that the water-temperature stratification was predicted well during this period, and the diurnal variation of stratification in the lake along the time axis is presented. Overall, the calculated values show good correlation to the observed values, while the temperature difference between the surface layer and the bottom layer is slightly underestimated. The largest water-temperature error in Case-FSW occurred around September 10th and was approximately 1 °C. A high RMSE of 0.97 and R^2 of 0.53 were also found during the research period, which further confirms the predictive capability of the model.

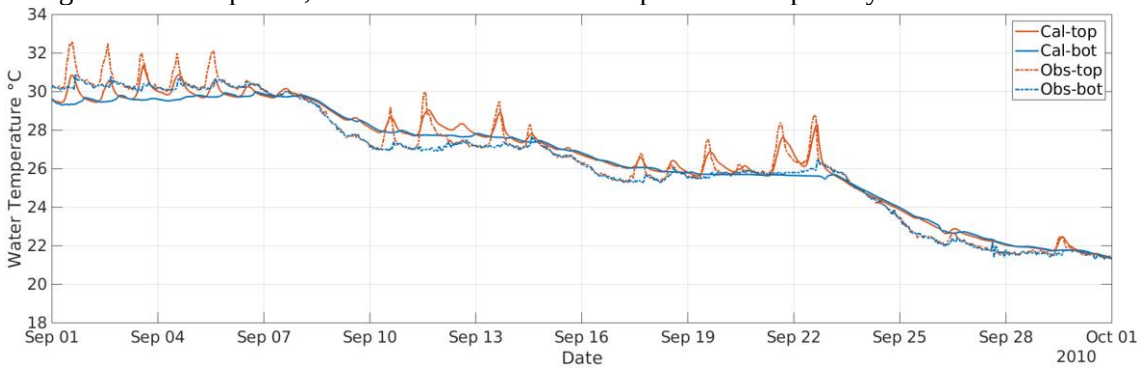

Figure 4. Comparison of calculated results and observed data at Koshin.

4.2 Discussion of external forces

Asou Station was chosen to illustrate the wind effect because the water depth here is only 1.5 m, which means it is has a stronger influence from winds than other stations. Figure 5 implies that the water-temperature stratification in Case-FS still appears in the calculation results. However, this was not seen in observations except for two very short periods around September 22nd. Meanwhile, the overall calculated value is larger than the observed value. The result shows that wind has the function of cooling the lake water. Additionally, it can promote vertical mixing in shallow areas, weakening the temperature stratification.

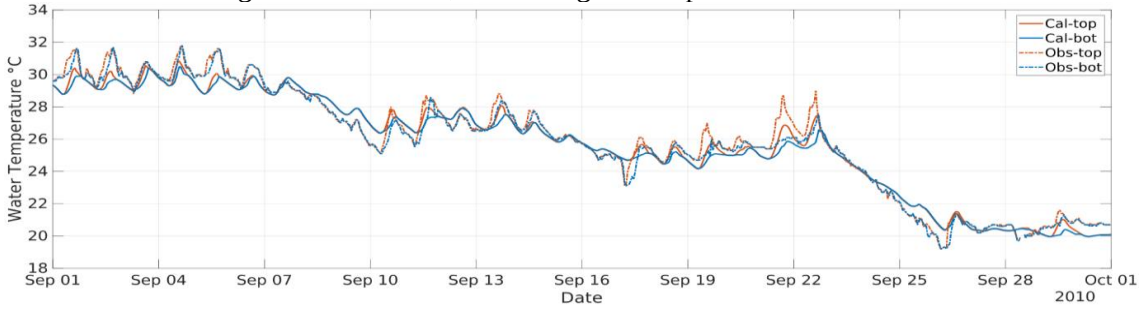

(a) Asou - Case-FSW

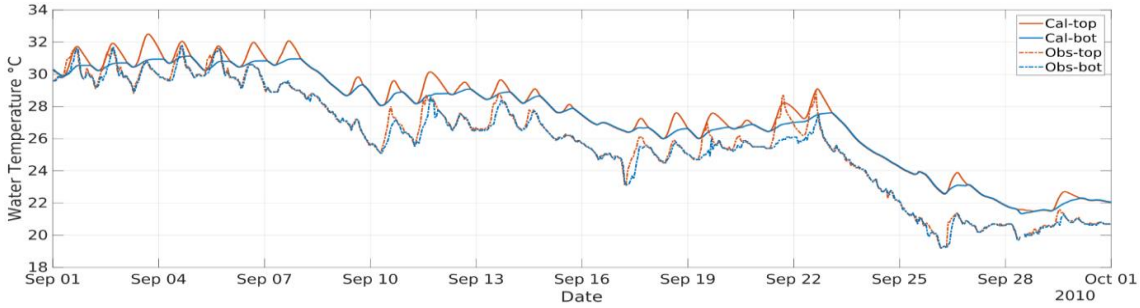

(b) Asou - Case-FS

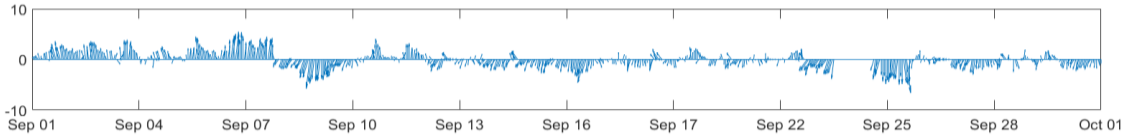

(c) Wind condition

Figure 5. Comparison of simulation results of Case-FSW (a) and Case-FS (b). The wind conditions over the same period are shown in (c).

Figure 6 shows the temporal change in water temperature at Koshin Station in Case-FSW and Case-FW. In Case-FW, there is a small temperature difference between the surface layer and the bottom layer on September 12th and 22nd; there are no temperature-stratification phenomena in other periods. The calculation results are generally lower than the observed values, although the downward trend is consistent with the

observed values. This shows that insolation has the function of warming the lake water. The overall impact, however, is not as great as that of air temperature factors. Temperature decisively affects the increasing or decreasing trend of lake water temperature. However, the amount of insolation plays an indispensable role in the formation of water-temperature stratification, mainly affecting the heat budget at the surface of the lake.

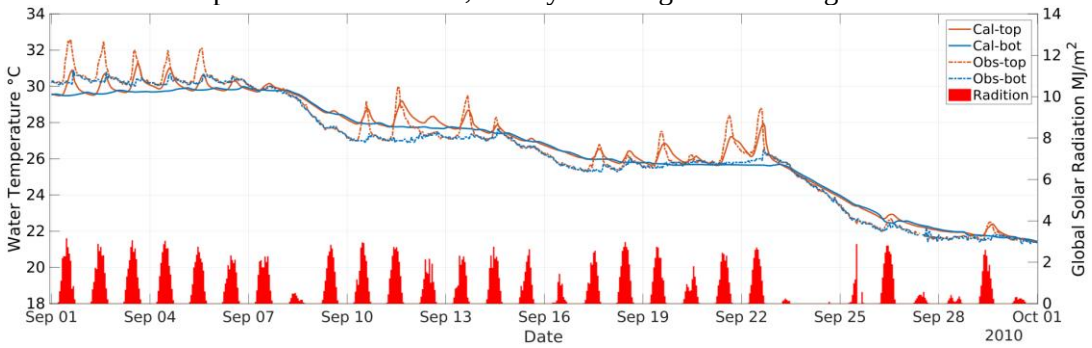

(a) Koshin - Case-FSW

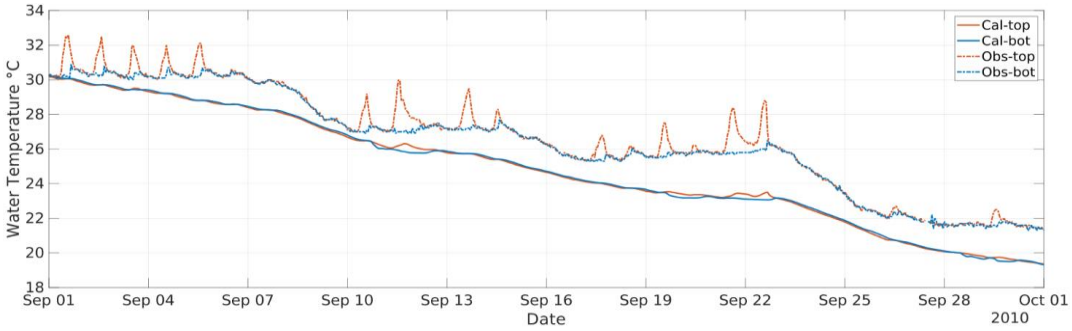

(b) Koshin - Case-FW

Figure 6. Comparison of simulation result of Case-FSW (a) and Case-FW (b).

During the research period, the inflow water temperature is higher than the original lake water. The difference in the spatial distribution of temperature between Case FSW and SW shows that the inflow of rivers plays a role in heating the water temperature, especially in the surface layer near the river mouth. This kind of effect is more obvious at Hirayama and Kakeuma, and inversely correlated with the distance from the inflow point.

4.3 Partial-tracking results

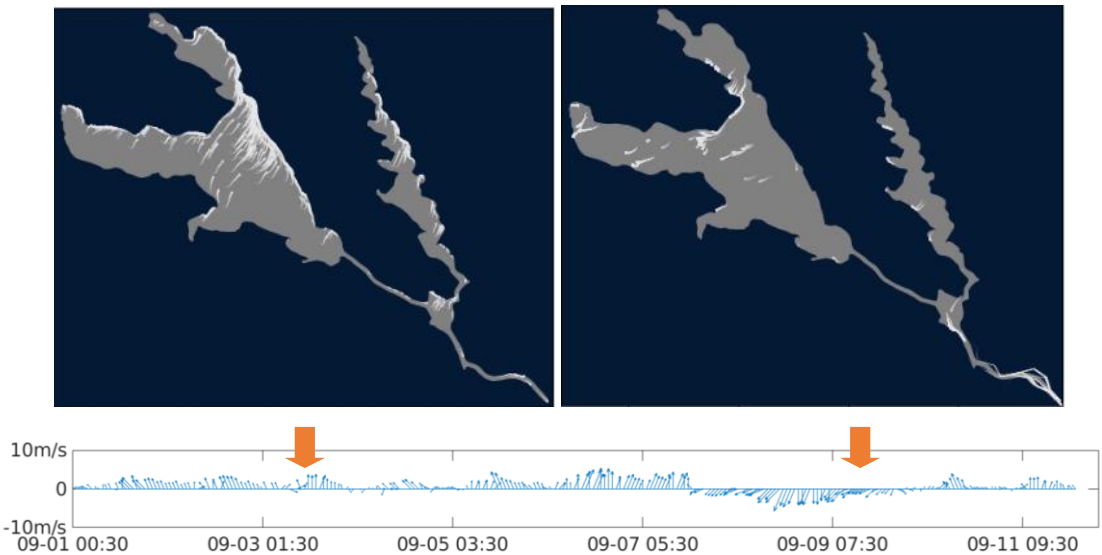

Figure 7. The results of particle tracking on September 3 and September 9. The figure below shows the wind condition at those times.

The lake is highly influenced by the sea breeze from the Pacific. During summer, southeasterly winds prevail over this region, while during winter, the winds turn to the northwest over most of the region. To illustrate the wind effects on surface substance transport, tracer simulations were performed for the same research period. Particle-tracking results are presented by animation; Figure 7 shows the results at two time-steps in the calculation period. The image on the left side is taken at 8 p.m. on September 3rd. After a long period of southerly wind dominance, surface particles moved northward to the northern shoreline of the lake and accumulated. On the right side, we could see that after approximately six days, surface particles recovered

slightly to the south due to dominant northerly winds, while there were still some particles trapped in lakeshore areas due to the complex shape of the lakeshore. The result is consistent with Islam (2013) who reported historical scenarios and the location of toxic cyanobacteria blooms in the lake.

5. CONCLUSIONS

In this study, numerical simulation using the SUNTANS simulator was performed for Lake Kasumigaura to simulate flow and temperature with attention to mixing and vertical stratification. From the results obtained, the applicability of the SUNTANS model in the lake was evaluated and significant influences of external forces that affect the distributions in the model were investigated.

The simulation results show that SUNTANS can reproduce field observations for the lake. Meanwhile, compared with the basic scheme, the accuracy of the results by introducing the preconditioning calculation has been improved. The model calculated results show a good performance for the obvious diurnal stratification. Through a comparison of results in different simulation scenarios, the driving effects of wind and the significant contribution of insolation to temperature stratification have been preliminarily understood. Additionally, it can be said that particle-tracking simulation can provide a suitable tool for revealing wind-driven current effects on the material cycles. From the results of particle-tracking simulation, the surface particles have a good response to the wind direction. In addition, due to the special and complex topographic structure of the lake, the aggregation of surface particles has been observed at certain locations. This characteristic is also considered as one of the reasons for the frequent occurrence of algal blooms in those regions.

ACKNOWLEDGMENTS

We thank Ministry of Land, Infrastructure, Transport and Tourism of Japan which continuously monitor river and water quality and provided extensive and quality data. A part of this work was supported by JSPS KAKENHI Grant Number 17K06576.

REFERENCES

Auger, G., & Wells, J. C. (2016). Gyre generation after a typhoon-induced upwelling in a stratified lake. In International Symposium on Stratified Flows (Vol. 1, No. 1).

Belolipetsky, Pavel V., et al. "Numerical modeling of vertical stratification of Lake Shira in summer." Aquatic ecology 44.3 (2010): 561-570.

Callisto, Marcos; Molozzi, Joseline and Barbosa, José Lucena Etham (2014). Eutrophication of Lakes

Chua VP, Fringer OB (2011) Sensitivity analysis of three-dimensional salinity simulations in North San Francisco Bay using the unstructured grid SUNTANS model. Ocean Model 39(3):332-350

Doudoroff, P., & Shumway, D. L. (1970). Dissolved oxygen requirements of freshwater fishes.

Fringer, O. B., Gerritsen, M., & Street, R. L. (2006). An unstructured-grid, finite-volume, nonhydrostatic, parallel coastal ocean simulator. Ocean Modelling, 14(3-4), 139-173.

Galperin, B., Kantha, L.H., Hassid, S., Rosati, A., 1988. A quasi-equilibrium turbulent energy model for geophysical flows. J. Atmos. Sci 45, 55–62.

Islam, M. N., Kitazawa, D., Hamill, T., & Park, H. D. (2013). Modeling mitigation strategies for toxic cyanobacteria blooms in shallow and eutrophic Lake Kasumigaura, Japan. Mitigation and adaptation strategies for global change, 18(4), 449-470.

Jin, Kang-Ren, John H. Hamrick, and Todd Tisdale. "Application of three-dimensional hydrodynamic model for Lake Okeechobee." Journal of Hydraulic Engineering 126.10 (2000): 758-771.

Kimura, Nobuaki, et al. "Diurnal dynamics in a small shallow lake under spatially nonuniform wind and weak stratification." Journal of Hydraulic Engineering 142.11 (2016): 04016047.

Kitazawa D., Komatsu N. (2008). Numerical Analysis of Stratification in Lake Kitaura. Seisankenkyu 60(1):51-54,

Komatsu, N., Ishii, Y., Watanabe, K., Homma, T., & Kitazawa, D. (2010). Field observation and analyses of oxygen-deficient water mass in Lake Kasumigaura. Annual Journal of Hydraulic Engineering, JSCE, 54, 1399-1404.

Masunaga, E., Fringer, O. B., & Yamazaki, H. (2016). An observational and numerical study of river plume dynamics in Otsuchi Bay, Japan. Journal of oceanography, 72(1), 3-21.

Mellor, G.L., Yamada, T., 1982. Development of a turbulence closure model for geophysical fluid problem. Rev. Geophys. Space Phys. 20, 851–875.

Rayson MD, Gross ES, Fringer OB (2015) Modeling the tidal and sub-tidal hydrodynamics in a shallow, micro-tidal estuary. Ocean Model 89:29-44

Sasaki K. (1993). Material circulation and bio-production in Inner Bay and tidal flats-3- Formation mechanism of hypoxia. Aquabiology, 15(3), p170-177.

Stepanenko, Victor, et al. "Simulation of surface energy fluxes and stratification of a small boreal lake by a set of one-dimensional models." Tellus A: Dynamic Meteorology and Oceanography 66.1 (2014): 21389.

Thiery, W. I. M., et al. "LakeMIP Kivu: evaluating the representation of a large, deep tropical lake by a set of one-dimensional lake models." Tellus A: Dynamic Meteorology and Oceanography 66.1 (2014): 21390.